This article was downloaded by:
On: *25 January 2011*
Access details: *Access Details: Free Access*
Publisher *Taylor & Francis*
Informa Ltd Registered in England and Wales Registered Number: 1072954 Registered office: Mortimer House, 37-41 Mortimer Street, London W1T 3JH, UK

Liquid Crystals
Publication details, including instructions for authors and subscription information:
http://www.informaworld.com/smpp/title~content=t713926090

Ising wall instability in a nematic liquid crystal

C. Chevallard[a]; M. Nobili[b]; J. -M. Gilli[a]
[a] (U.M.R. 129 CNRS/UNSA) Université de Nice Sophia-Antipolis, Institut Non-Linéaire de Nice, 1361 route des Lucioles, 06560 Valbonne, France, [b] Groupe de Dynamique des Phases Condensées-CC26 (U.M.R. 5581 CNRS/UMII) Université Montpellier II, 34095 Montpellier Cedex 5, France,

Online publication date: 06 August 2010

To cite this Article Chevallard, C. , Nobili, M. and Gilli, J. -M.(2001) 'Ising wall instability in a nematic liquid crystal', Liquid Crystals, 28: 2, 179 — 189
To link to this Article: DOI: 10.1080/02678290010003705
URL: http://dx.doi.org/10.1080/02678290010003705

PLEASE SCROLL DOWN FOR ARTICLE

Full terms and conditions of use: http://www.informaworld.com/terms-and-conditions-of-access.pdf

This article may be used for research, teaching and private study purposes. Any substantial or systematic reproduction, re-distribution, re-selling, loan or sub-licensing, systematic supply or distribution in any form to anyone is expressly forbidden.

The publisher does not give any warranty express or implied or make any representation that the contents will be complete or accurate or up to date. The accuracy of any instructions, formulae and drug doses should be independently verified with primary sources. The publisher shall not be liable for any loss, actions, claims, proceedings, demand or costs or damages whatsoever or howsoever caused arising directly or indirectly in connection with or arising out of the use of this material.

LIQUID CRYSTALS, 2001, VOL. 28, NO. 2, 179–189

Ising wall instability in a nematic liquid crystal

C. CHEVALLARD*, M. NOBILI† and J.-M. GILLI
Institut Non-Linéaire de Nice,
(U.M.R. 129 CNRS/UNSA) Université de Nice Sophia–Antipolis,
1361 route des Lucioles, 06560 Valbonne, France
†Groupe de Dynamique des Phases Condensées-CC26
(U.M.R. 5581 CNRS/UMII) Université Montpellier II,
34095 Montpellier Cedex 5, France

(*Received 20 October 1999; in final form 12 July 2000; accepted 12 July 2000*)

A new instability for a splay-bend Ising wall was found in a 5CB nematic liquid crystal layer. This instability, which occurs in the presence of an external horizontal magnetic field, is driven by the elastic anisotropy of the liquid crystal material. Depending on the homogeneity of the magnetic field, the unstable straight interface evolves towards a new steady state or undergoes a spinodal decomposition into facets. Energy arguments are given in order to explain these physical phenomena.

Downloaded At: 18:12 25 January 2011

1. Introduction

The nematic liquid crystal phase is an anisotropic phase of matter. In its lowest-energy state, the molecules are, on average, oriented along a preferred direction specified by a vector **n** called the *director*. An elastic energy is associated with any deviation from this uniform state, that is, with any spatial inhomogeneity of the director orientation. As a consequence of the anisotropic properties of liquid crystals, this elastic energy depends on three different elastic constants, namely the splay K_1, the twist K_2 and the bend K_3 constants, which account for three different kinds of director distortions [1]. Generally, the elastic anisotropy of nematic liquid crystals does not strongly affect the physical phenomena. For a qualitative understanding of experimental observations, one can use the one-constant approximation, which reads $K_1 = K_2 = K_3 = K$. Such an approximation seems rather sensible in view of the actual values of the three elastic constants for most of the usual nematic compounds. Considering the elastic anisotropy becomes therefore really useful when one is trying to fit the experimental data quantitatively.

In some cases nevertheless, the one-constant approximation must be discarded since it does not allow a correct description of the physical phenomena. This happens in two major situations: either the nematic compounds are strongly anisotropic, or strongly distorted regions are present in the nematic medium.

*Author for correspondence;
e-mail: fecheval@wisemail.weizmann.ac.il

The first situation is encountered with polymer nematics such as PBG (polybenzylglutamate, $K_1/K_2 \sim 15$), which are composed of very long molecules. This gives rise to an *inhomogeneous* Fréedericksz transition [2], which yields the emergence of a periodic modulated phase in place of the homogeneous tilted one usually observed in the splay (planar) geometry of the Fréedericksz transition. The transition to a modulated phase can also be seen in the vicinity of the nematic–smectic A transition due to the divergence of the twist and bend elastic constants [3]. Because the twist constant diverges more slowly than the bend constant, the Fréedericksz instability in the bend geometry favours a state which involves some twist distortion in place of the bend distortion. This leads to the appearance of a periodic modulated state.

Besides, the elastic anisotropy, even small, changes the equilibrium configuration of strongly distorted regions of the nematic phase, namely defects like singular points or lines, umbilics and walls. For most of the usual compounds, the twist constant is about half the splay and bend constants. As a consequence, twist distortions are energetically favoured with respect to splay and bend deformations. This explains that a pure splay (+1)-vortex is unstable towards a partially twisted one [4]. Moreover, this results in a high energy barrier to be overcome during a twist–splay–twist transition of the defect, and accounts for the step-like unwinding process observed in smectic films during the relaxation of the spiral pattern developed around a (+1)-umbilic [5]. Both comments, on static configuration and unwinding process, also apply to the singular defect located at the

Liquid Crystals ISSN 0267-8292 print/ISSN 1366-5855 online © 2001 Taylor & Francis Ltd
http://www.tandf.co.uk/journals
DOI: 10.1080/02678290010003705

centre of a nematic droplet (see [1], p. 187, for static configuration, and [6] for relaxation). The emission of waves from the core of a dynamic spiral [7] follows from the same last effect. In this experiment, the periodic twist–splay–twist transformation of the umbilic is driven by a rotating horizontal magnetic field. Due to the existing energy barrier, the phase of the defect is locked for a while and then relaxes thanks to a π-wall. Furthermore, and because they involve different kind of distortions, (+ 1) and (− 1) umbilics have different energies, and therefore different sizes. As a consequence, dynamical spirals developed around (+ 1) and (− 1) vortices differ in their pitch by up to 20% [8].

Singular lines and walls configurations are also affected by the elastic anisotropy. Thus, one can demonstrate that (± 1/2) wedge disclinations are unstable towards a twist disclination involving an escape of the director in the direction of the line (this leads to the zigzagging lines observed [9]). Lastly, the measurement of the ellipticity of looped walls [10] provides a good estimate of the elastic ratio K_2/K (under the assumption $K_1 = K_3 = K$).

To conclude, one can remark that the instability from straight to oblique rolls in a convective situation originates from the elastic anisotropy of the nematic material [11].

In this paper, we present the zigzag-like instability of an Ising wall and show that it is driven by the elastic anisotropy of the nematic compound used, namely the 4-pentyl-4′-cyanobiphenyl (5CB). For such a material, the elastic anisotropy is weak and therefore not sufficient to induce an inhomogeneous Fréedericksz transition. However, the existence of strong distortions in the system, associated with the presence of an Ising wall, enhances the effect of the elastic anisotropy and possibly results in the wall instability. A qualitatively similar instability, but in a different geometry, has already been reported by Cramer *et al.* [12]. Such a 'zig-zag' instability looks like the phase instability that distorts the structures of straight rolls in the Rayleigh–Bénard convection [13] or in the electroconvection of anisotropic fluids [14]. It can also be observed in crystal growth where it affects the front between the two competing thermodynamic phases [15, 16]. Lastly, a similar instability has been noticed to occur on the interface separating two domains of opposite 'chevron' structures in smectic liquid crystal films [17].

A dynamic approach for this 'zigzag' instability has already been developed [18]. This last study provides a quantitative description of the Ising wall instability near the Fréedericksz transition, in the framework of bifurcation theory. In the present paper, we shall emphasize the experimental aspects and develop an explanation, based on energy arguments, of the observed phenomena. In the first section we present the experimental set-up used for all experiments. In § 2 we describe the instability and show how its nature depends on the homogeneity of the magnetic field. Experimental data are presented in § 3. Finally a theoretical explanation of the zigzag instability, based on the Frank free energy, is given in § 4.

2. Experimental set-up

In this paper, we shall consider the homogeneous Fréedericksz transition that occurs in a homeotropic liquid crystal cell. All experiments have been realized using the nematic 5CB compound. Both its dielectric ε_a and diamagnetic χ_a anisotropies are positive. The Fréedericksz transition is induced by applying a horizontal magnetic field to the sample. This results in a splay–bend deformation of the director in a vertical plane containing the magnetic field. Owing to the twofold degeneracy of the bifurcated state, domains of opposite (re-)orientation are created [19]. The interface between two of these domains is called an Ising wall [20]. Starting from a straight splay–bend Ising wall, a zigzag-like instability develops. We shall see that this instability arises because of the liquid crystal elastic anisotropy.

The 5CB compound is in the nematic phase at room temperature. Its anisotropic physical properties are well characterized by the following constants, at $T = 25°C$: elastic constants [21] $K_1 = 6.3$, $K_2 = 4.1$, $K_3 = 8.4$ (10^{-7} dynes); dielectric anisotropy [22] $\varepsilon_a = 11.3$; diamagnetic anisotropy [23] $\chi_a = 1.142$ (10^{-7} cm^3 g^{-1}); rotational viscosity $\gamma_1 \sim 10^{-2}$ Pa s. The cells are made of two conductive ITO (indium tin oxide) glass plates separated by thin mylar spacers which set the thickness d of the cell. This thickness can be varied over the range 50–150 μm. The glass surfaces are treated with lecithin to provide a homeotropic anchoring (director perpendicular to the glass plates). A vertical electric field $\mathbf{E} = E\mathbf{z}$ ($V_{\text{eff.}} \sim 0$–9 V) is applied. The use of a high frequency (~ 5 kHz) a.c. electric field protects the system from charge injection or electroconvection phenomena. Two permanent magnets are used to produce a horizontal magnetic field $\mathbf{H} = H\mathbf{x}$ up to 0.7 T. The 5CB sample can be placed either in the inhomogeneous field region or in the area between the two magnets where the magnetic field is uniform (see figure 1). In the inhomogeneous region, the magnetic field is characterized by a linear variation of the vertical component along the x-axis. More precisely, for all experiments that involved an inhomogeneous magnetic field, the gradient of vertical component is about 5.10^{-2} T mm^{-1} (this will result in a variation of about 10^{-3} T of the vertical magnetic component over the wall thickness at the onset of the zig-zag instability).

Downloaded At: 18:12 25 January 2011

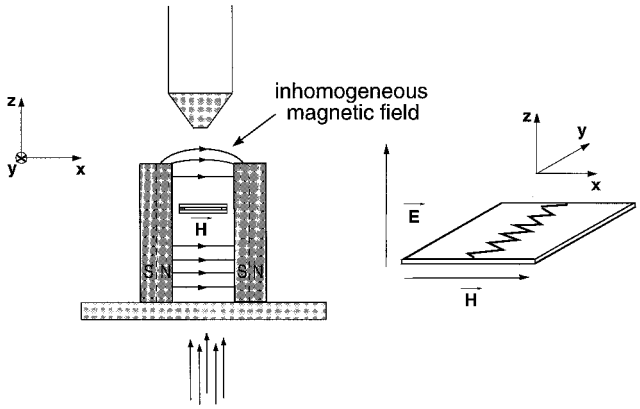

Figure 1. Experimental set-up.

Following our choice of the nematic compound and cell geometry, the Fréedericksz transition is induced by the horizontal magnetic field, whereas the vertical electric field stabilizes the initial homeotropic state. A splay–bend Ising wall [10] is formed by placing the cell in the inhomogeneous magnetic field region (see figure 1). Its width is determined by the distance to the Fréedericksz threshold and can be modified by change of the field magnitudes. All experimental observations are made through a polarizing microscope. Video films and numerical images (see figure 2) are recorded by a 3CCD camera placed on the top of the microscope.

3. Instabilities of an Ising wall in a magnetic field

3.1. *Instability in a magnetic trap*

In the experiment described below, the sample of liquid crystal is always kept in the *inhomogeneous* region of the magnetic field. For some values of the electric and magnetic fields, that put the system beyond the threshold of the Fréedericksz instability, a single splay–bend Ising wall appears in the nematic cell. This wall forms at the position of null magnetic field gradient (see figure 1) which acts as a restoring force around this particular position.

One then starts to decrease the amplitude of the stabilizing electric field in order to make the interface thinner and thinner. This process enhances the elastic distortions inside the wall. For large enough distortions (and so, rather far from the Fréedericksz threshold), the

Downloaded At: 18:12 25 January 2011

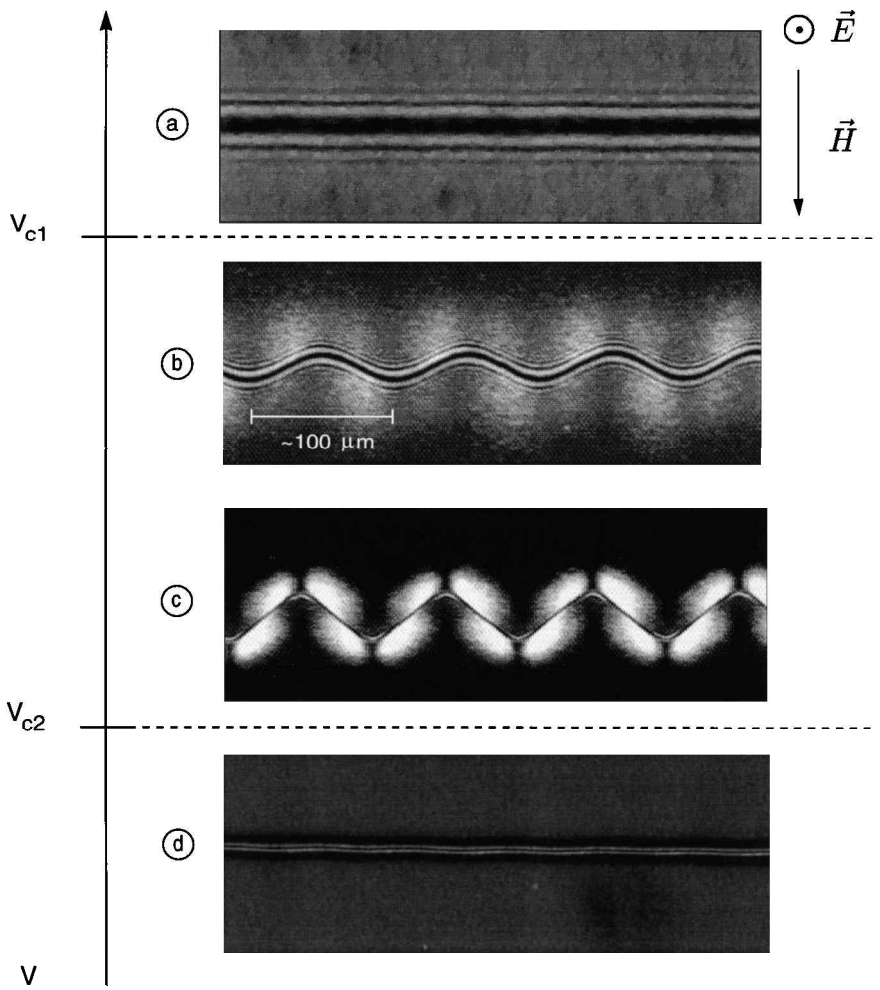

Figure 2. Experimental photographs of the Ising wall instability: for $V > V_{c_1}$ or $V < V_{c_2}$, the straight Ising wall is stable, see images (*a*) and (*d*); for $V_{c_1} > V > V_{c_2}$ the straight interface is unstable versus a periodically shaped, sinusoidal or faceted, interface, see images (*b*) and (*c*).

straight wall becomes unstable. Its destabilization drives the system towards a new stable stationary state characterized by a periodic shape of the interface (see figure 2). Near the instability threshold, the Ising wall shows a sinusoidal profile, figure 2 (*b*). If the voltage is further decreased, the interface reaches a periodic faceted shape, figure 2 (*c*). The straight wall is eventually restabilized by decreasing the voltage later, figure 2 (*d*). This last observation indicates that the effective control parameter of the instability is a non-linear function of the electric field. In some cases however, it is not possible to observe this restabilization because the wall undergoes a decomposition into two singular lines (figure 3) that nucleate at the edges of the sample.

The previous instability, undergone by the splay–bend Ising wall in the presence of an inhomogeneous magnetic field, occurs without any visible hysteresis. Moreover, experimental observations indicate that, in the new stable state, the director escapes the magnetic plane (x, z) in the neighbourhood of the interface. That can actually be deduced from observations using crossed polarizers, one of them being parallel to the magnetic field. When it is straight, the splay–bend Ising wall looks dark through the polarizing microscope, since the director lies everywhere in the magnetic plane. Following the destabilization of the straight interface, one can see light reappear on both sides of the wall, see for example figure 2 (*c*). This reveals the escape of the director from the magnetic plane.

In order to determine the structure of the wall, we added to the optical path a waveplate turned by 45° with respect to the polarizers axes (see figure 4). Analysis of the birefringence colours shows that the escape of the director inside the zig and zag regions occurs in opposite direction, in a way that tends everywhere to make the director parallel to the interface. All these observations lead to the determination of the new wall structure beyond the instability threshold (figure 5). As shown in figure 5, the wall destabilization has two main features. First, it corresponds to a local reorientation of the wall; second it brings the wall into a new structure in which the splay distortion has been partially replaced by some twist distortion. In this new steady state, the gain in elastic energy, due to the local rotation of the wall and to the director reorientation, is balanced by the energy cost associated with the interface elongation and the escape of the director from the magnetic plane.

These results point out the elastic anisotropy as the key factor of the destabilization. Such a result is not surprising if one remembers that the free energy per unit length of a pure twist wall is lower than the one of a splay–bend wall for compounds similar to 5CB [10].

Downloaded At: 18:12 25 January 2011

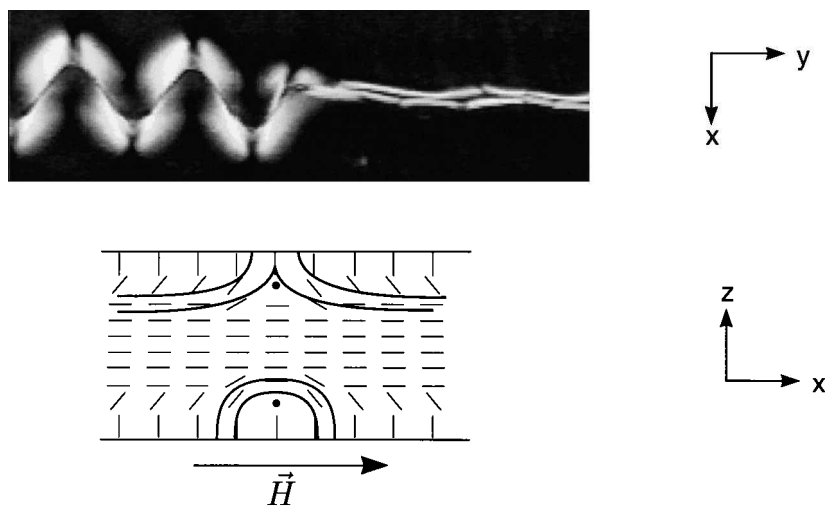

Figure 3. Wall decomposition into singular lines.

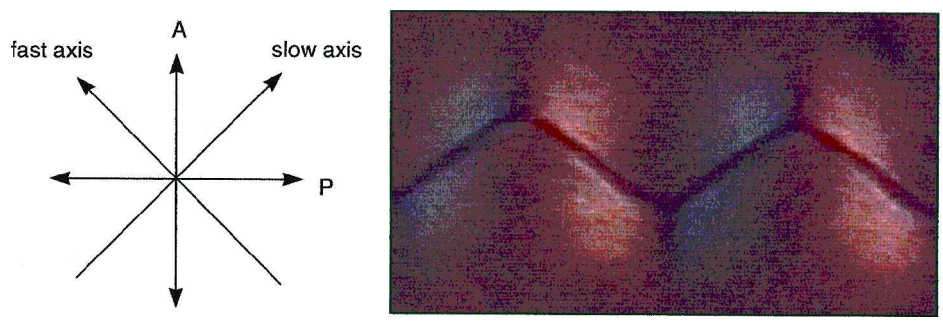

Figure 4. Use of a waveplate to determine the new structure of the wall beyond the instability threshold.

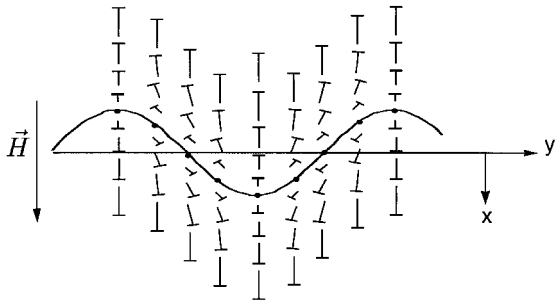

Figure 5. Structure of the wall beyond the zigzag instability: the wall destabilization corresponds first to a local rotation of the interface, second to a change of the inside structure of the wall.

Besides, it is known that a wall, formed in a planar geometry and turned by a non-zero angle with respect to the external field, may reduce its energy by choosing a configuration in which the director escapes the vertical plane defined by the external field [24].

3.2. *Zigzag instability of an Ising wall in a homogeneous magnetic field*

We now present the experimental results concerning the Ising wall instability in the presence of a *homogeneous* magnetic field.

An Ising wall in the splay-bend configuration is formed in the region where the field is inhomogeneous (see figure 1) and then quenched into the area between the two magnetics where the field is homogeneous. Near the Fréedericksz threshold it is very difficult to keep the wall in an average position between the two magnets, since any imperfection in the parallelism between the sample and the plane of the magnetic field makes the wall drift towards one edge of the cell. Therefore the experiments have been carried out rather far from this threshold.

As long as its width is larger than a critical size, the splay–bend Ising wall is always unstable when it is thrust into the homogeneous area of the magnetic field. It first develops a spatial oscillation, and later loses its sinusoidal shape towards a faceted line composed of pieces of wall turned by an angle $\pm \Psi_0$ (see figure 6). This faceted wall looks like the faceted propagating front observed in some crystal growth experiments [15, 16] for a strongly anisotropic crystal. Thus, in directional solidification, a zigzag instability (known as the Herring's instability by metallurgists) can occur if one forces the growth of the crystal in a forbidden direction. However, one must note that, contrarily to the solidification front, the Ising wall does not propagate since it separates two energetically identical states.

Two adjacent pieces of the faceted wall, whose orientations are opposite, are connected by a region of strong curvature that we shall call a 'kink' [18]. The dynamics that follows the destabilization of the wall, consists in gathering the domains of same orientation, the angles of the 'zig' and 'zag' facets staying unchanged. This process occurs thanks to annihilations of kinks and without any characteristic length scale. Indeed, the average size of the domains increases monotonically in time (see figure 6). The dynamics, which tends to separate the zig and zag states, resembles the one-dimensional counterpart of the spinodal decomposition dynamics observed in conservative binary mixtures [25]. The two kinds of facets, characterized by their tilt with respect to the initial direction of the wall, are the analogues of the two types of domains, characterized by different concentrations, present in the phase separation process of binary mixtures. In both cases, the spinodal decomposition involves coarsening dynamics, that is interaction and annihilation of defects (kinks).

These experimental observations clearly highlight the role of the magnetic gradient in the experiments

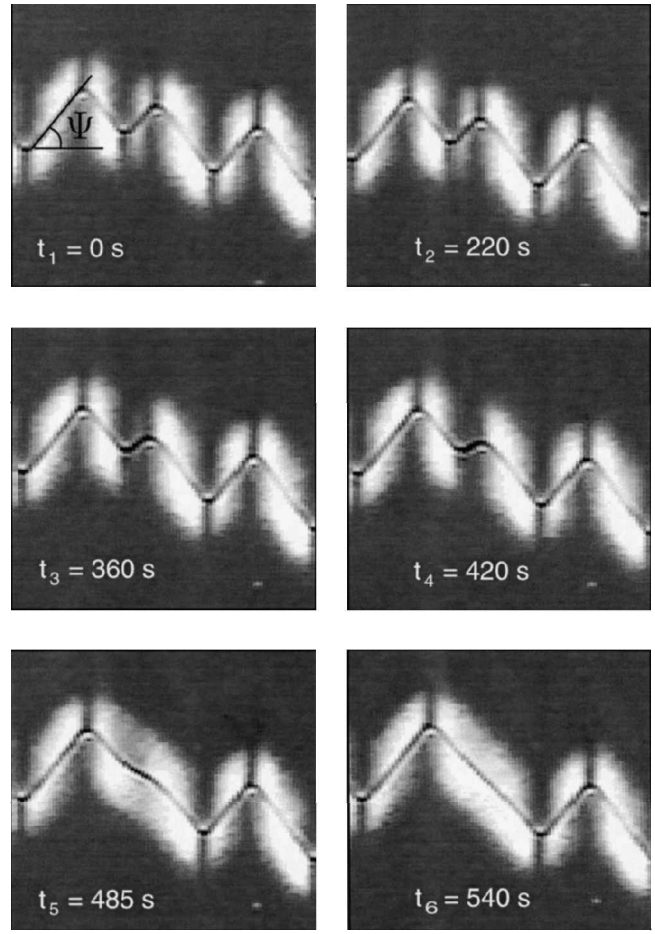

Figure 6. Spinodal decomposition of the wall in a homogeneous magnetic field.

Downloaded At: 18:12 25 January 2011

described previously in § 3.1: it stabilizes the straight splay–bend configuration of the wall and, when this one becomes eventually unstable, saturates the instability. The magnetic field gradient is therefore an antagonistic effect to the elastic anisotropy that triggers the instability.

4. Theoretical development

4.1. *Quantitative features for the destabilized wall*

It is relevant to determine the dimensionless control parameters of the instability. This can easily be done, without any calculation, by looking at the free energy expression. The Frank free energy density of a nematic sample subjected to some external magnetic and electric fields, reads [1, 4]

$$F = \frac{1}{2}\{K[(\mathrm{V}\mathbf{n})^2 + (\mathbf{n}\times(\mathrm{V}\times\mathbf{n}))^2] + K_2[\mathbf{n}\ (\mathrm{V}\times\mathbf{n})]^2 - \varepsilon_a(\mathbf{n}\ \mathbf{E})^2 - \chi_a(\mathbf{n}\ \mathbf{H})^2\}. \quad (1)$$

In equation (1) we have used the two-constants approximation $K_1 = K_3 = K \neq K_2$; $\mathbf{n} \equiv (\sin\theta\cos\phi,\ \sin\theta\sin\phi, \cos\theta)$ is the director (see figure 7). The stabilizing electric field $\mathbf{E}$ is directed along the normal $\mathbf{z}$ to the glass plates, $\mathbf{E} \equiv (0, 0, E)$, and the magnetic field $\mathbf{H}$ is parallel to the x-axis, $\mathbf{H} \equiv (H, 0, 0)$. The elastic part in the free energy equation (1) depends on K and on the elastic anisotropy $\delta k = K_2/K$.

The magnetic and electric terms in the free energy (1) can be written as:

$$F_{mag} + F_{élec.} = -\frac{1}{2}\chi_a H^2 + \frac{1}{2}[\chi_a H^2 - \varepsilon_a E^2]\cos^2\theta + \frac{1}{2}\chi_a H^2 \sin^2\theta\sin^2\phi. \quad (2)$$

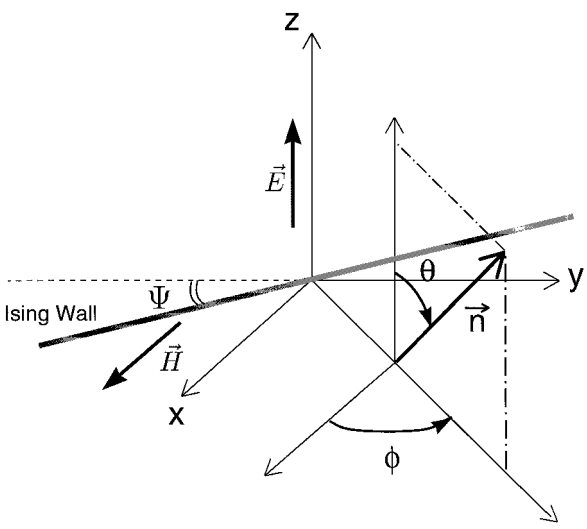

Figure 7. Definition of the director coordinates θ and ϕ.

In the above expression, we can ignore the first term which is independent of the director orientation. The second term can be combined with the elastic term, considering that $\chi_a H^2 - \varepsilon_a E^2 = K/\xi^2$ far from the Fréedericksz threshold. ξ is the magneto-electric coherence length and gives a scale for the Ising wall thickness. The last term in equation (2) expresses the energy cost resulting from the escape of the director from the magnetic plane (x, z). This term produces a restoring force that tends to put the wall back into the splay–bend configuration. From the last term in equation (2) one can define another characteristic length scale, namely the magnetic coherence length ξ_H, which satisfies $\chi_a H^2 = K/\xi_H^2$. ξ_H represents the typical size of the region where the director escapes the magnetic plane. Its precise definition is explained in figure 8: ξ_H is the length of the distorted region in a semi-infinite medium whose bulk is uniformly oriented by a magnetic field and whose boundary is anchored perpendicularly to the magnetic field. Therefore, in our problem, its value follows the magnitude of the restoring force exerted by the magnetic field on the director. Figure 9 shows the meaning of the two characteristic length scales for the experimental situation under study.

For the sake of simplicity we shall consider, in the analysis below, a wall which is globally turned by an angle Ψ with respect to the y-axis. Its position P along this axis is expressed by $P = y\tan\Psi + cst$ (see figure 7) where cst denotes an additive constant that takes into account the translational invariance of the system along the x-axis. We assume that the director angles θ and ϕ do not depend on the distance z from the plates (bidimensional analysis).

From the two characteristic length scales, ξ and ξ_H, one can construct the dimensionless order parameter ξ/ξ_H. Besides, if one considers that the two angles θ and ϕ are of the general form $\theta = \Theta(x - P(y)/\xi)$ and $\phi = \Phi(x - P(y)/\xi)$, then the free energy per unit length along the y-axis, of a wall turned by an angle Ψ, reads:

$$f(\Psi) = \frac{K}{\xi}\left[A(\Psi, \delta k) + B(\Psi, \delta k)\frac{\xi^2}{\xi_H^2}\right].$$

A and B are two functions of the dimensionless control parameters $\delta k = K_2/K$ and ξ/ξ_H. Minimizing this energy with respect to Ψ leads to the two symmetrical states $\pm\Psi_0$ corresponding to the 'zig' and 'zag' facets. Ψ_0 depends on the two dimensionless parameters δk and ξ/ξ_H. This result allows expression of the experimental data in term of the relevant parameters of the problem.

The amplitude A and wavelength λ of the periodic steady shape versus the applied voltage have been plotted in figure 10. Here the cell thickness is $d = 157\,\mu\mathrm{m}$ and the sample is submitted to an inhomogeneous magnetic

Downloaded At: 18:12 25 January 2011

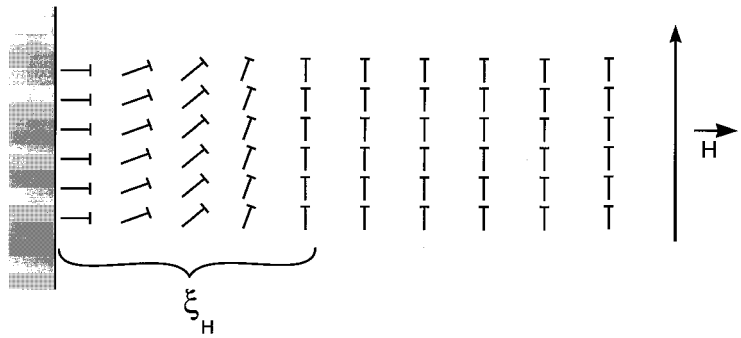

Figure 8. Definition of the magnetic coherence length: this length scale corresponds to the size of the reorientation domain in a semi-infinite medium whose bulk is uniformly oriented by a magnetic field and whose boundary anchoring direction is perpendicular to this field.

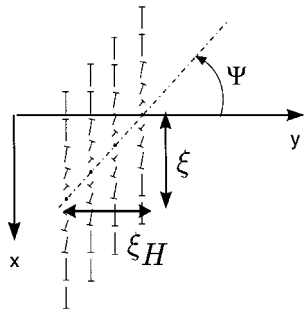

Figure 9. Meaning of the two characteristic length scales of the problem: the electro-magnetic coherence length ξ gives the size of the wall along the x-direction; whereas the magnetic coherence length ξ_H gives the ϕ-variation distance from the centre of the wall along the y-axis.

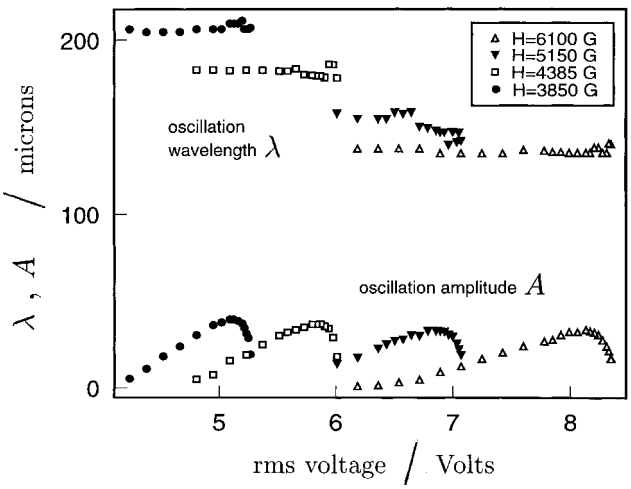

Figure 10. Experimental curves characterizing the destabilized wall for a sample whose thickness is $d = 157\,\mu$m and for different values of the magnetic field H. Apparently the spatial period of the wall depends only on the magnetic field. On the contrary the amplitude strongly depends on the electric voltage but nearly not on the magnetic field.

field. Different curves corresponding to different amplitudes of the horizontal magnetic field are represented. For a given magnetic field, the amplitude of the spatial oscillation is zero at the instability threshold (high voltage region) and then begins to increase for decreasing applied voltages. At intermediate voltages, the interface shape is no longer sinusoidal but rather faceted. If one further decreases the voltage, the amplitude, after reaching a maximum, starts to decrease and goes eventually to zero. Thus, the instability occurs over a finite range of voltages, whose width is about 2 V. Besides, the wavelength is almost constant over this range. This means that the wavelength does not depend on the electric field but only on the magnetic field. Since the gradient of vertical magnetic component over the sample is similar for all values of the horizontal magnetic field, the change in the wavelength value must be attributed to the change in the horizontal magnetic field component. In figure 11 both the amplitude and the wavelength have been plotted versus the dimensionless parameter ξ/ξ_H. A range of instability that is common to all values of magnetic field emerges from this scaling: ξ/ξ_H is indeed a control parameter for the instability.

In order to check the two-dimensional approximation (θ and ϕ independent on z), we have plotted in figure 12 the dimensionless quantity λ/ξ_H versus ξ/ξ_H for different cell thicknesses. Under such a scaling, the dimensionless wavelength gets a single value for all experiments. This value probably depends on the elastic anisotropy; that has not been changed in our experiments, but does not apparently depend on the cell thickness, as expected. Thus, the chosen two-dimensional analysis seems quite accurate to describe the system. This can be confirmed by comparing the electro-magnetic coherence length ξ with the cell thickness d. In our experiment $\xi/d \approx 1/10 \ll 1$. One can then consider that the director far from the Ising wall is completely aligned with the magnetic field and that a good description of the system can ignore the z-dependence of the director orientation angles θ and ϕ.

In the case of the spinodal decomposition, that is in the presence of a homogeneous magnetic field, the unstable state can be characterized by the slope P_y of the facets. By plotting this quantity versus ξ/ξ_H, one obtains the curve shown in figure 13. Two sets of experimental data, corresponding to two different samples, lie on the same straight line. This 'universal' curve depends

Downloaded At: 18:12 25 January 2011

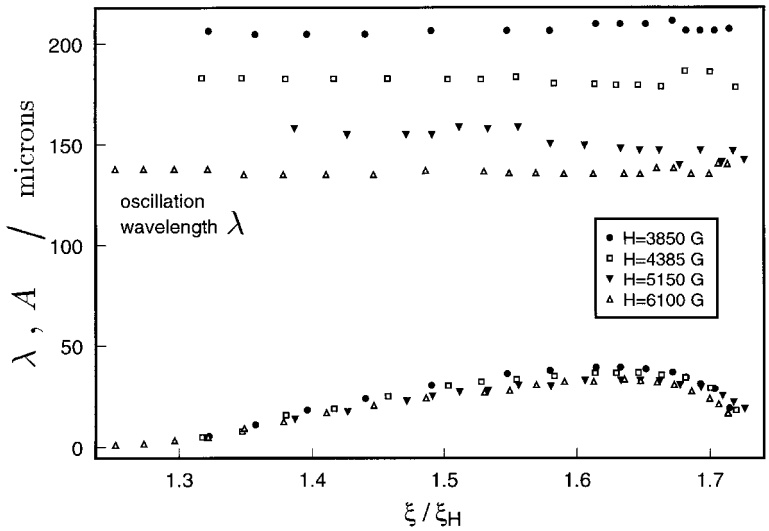

Figure 11. Same curves as those presented on figure 10 but versus the dimensionless quantity ξ/ξ_H values. The wavelength does not depend on this parameter but strongly changes with the magnetic field magnitude.

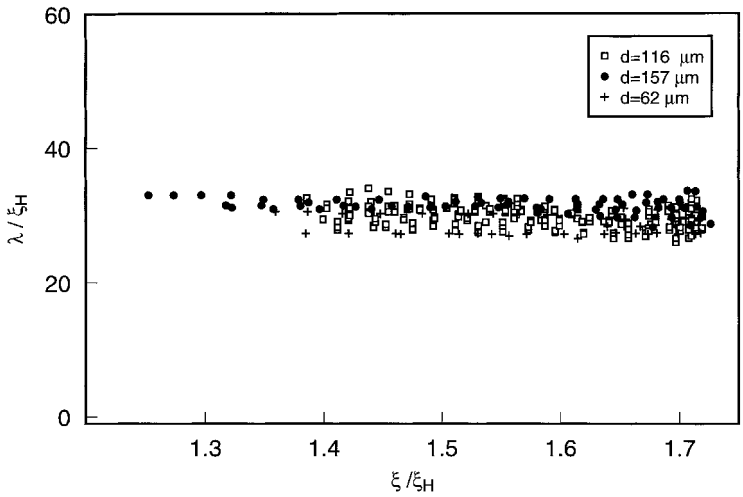

Figure 12. Wavelength, rescaled by the magnetic coherence length, versus the dimensionless parameter ξ/ξ_H.

Downloaded At: 18:12 25 January 2011

on the elastic anisotropy. The lack of data at lower values of ξ/ξ_H is due to some experimental difficulties. As already mentioned in § 3, the wall undergoes a decomposition into singular lines for small values of its thickness, i.e. for small values of ξ/ξ_H. This process initiates at the edges of the sample and then propagates along the wall, making the measurements very difficult. However, if one decreases the voltage fast enough, it can be seen, in the part of the wall not affected by this phenomenon, that the tilt angle of the facets further decreases and eventually cancels out for a critical value of the dimensionless parameter ξ/ξ_H. Therefore, the instability no longer occurs for small values of ξ/ξ_H, as actually suggested by an extrapolation of the curve in figure 14 at lower values of the control parameter. Then the elastic gain coming from the change in the wall structure is no longer sufficient to induce the rotation of the interface.

4.2. *Energy analysis*

In the homogeneous magnetic field, the wall instability leads to the emergence of two symmetrical states which are the zig and zag facets. The zig and zag facets are the two new minima of the free energy. We have made an energy calculation, with rather strong simplifying assumptions, to demonstrate the existence of these minima.

In view of this calculation, one must choose an *ansatz* that depicts the structure of the wall turned by an angle Ψ. We first assume that the director angles θ and ϕ do not depend on the z-coordinate (bidimensional analysis). This assumption seems reasonable, as discussed in the experimental section. Moreover, we assume that the escape of the director from the plane (x, z) is weak ($\phi \ll 1$ in figure 7) and that it happens over the same domain as the θ-variations across the wall (see figure 14). The θ-dependence is chosen of a hyperbolic form, which is

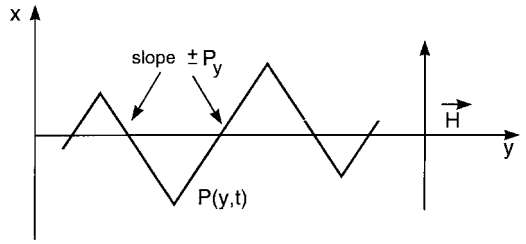

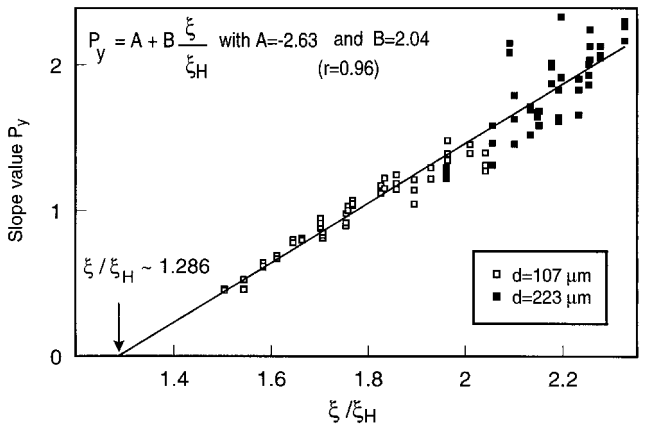

Figure 13. Characteristic of the unstable state for an Ising wall in a homogeneous magnetic field.

an exact description of the wall distortions near the Fréedericksz threshold. In the above saturated situation, a more realistic description would involve elliptic integrals but would complicate the analysis without giving any additional information. The ϕ-dependence is represented by an even function of x. Moreover ϕ must be zero for the two limit cases $\Psi = 0$ (splay–bend wall) and $\Psi = \pi/2$ (twist wall) and maximum in the intermediate case $\Psi = \pi/4$. The expression given below fulfils the preceding requirements and allows analytic calculations:

$$\theta(x, y, t) = -\frac{\pi}{2}\tanh\left[\frac{k(x + y\tan\Psi)}{(1 + \alpha^2\tan^2\Psi)^{1/2}}\right]$$

$$\phi(x, y, t) = -\frac{p\pi}{4}\sin(2\Psi)\,\mathrm{sech}^2\left[\frac{k(x + y\tan\Psi)}{(1 + \alpha^2\tan^2\Psi)^{1/2}}\right] \tag{3}$$

where $\alpha = (K_2/K_1)^{1/2}$ and $p \ll 1$ quantifies the escape of the director from the magnetic plane. The free energy of the system, linearized with respect to ϕ, reads:

$$F = \frac{1}{2}[K\theta_y^2 + K_2\theta_x^2 + 2(K - K_2)\theta_x\theta_y\phi + 2(K\theta_y\phi_x - K_2\theta_x\phi_y)\sin\theta\cos\theta - \chi_a H^2\sin^2\theta - \varepsilon_a E^2\cos^2\theta] \tag{4}$$

where one has used the two-constants approximation ($K_1 = K_3 = K \neq K_2$). The free energy per unit length of the wall along the y-axis is obtained by integrating the preceding equation over x:

$$f(\Psi) = (1 + \alpha^2\tan^2\Psi)^{1/2}\left[\frac{\pi^2}{6}kK + \frac{\beta}{k}(\chi_a H^2 - \varepsilon_a E^2)\right] - \frac{(45 - 2\pi^4)}{15\pi}kK(1 - \alpha^2)\frac{p\sin^2\Psi}{(1 + \alpha^2\tan^2\Psi)^{1/2}} \tag{5}$$

where $\beta = 0.609$.

Considering that $k^2 \sim [1/\xi^2 = \chi_a H^2 - \varepsilon_a E^2/K]$ for a strongly confined wall, one gets:

$$\frac{f(\Psi)}{kK} = A(1 + \alpha^2\tan^2\Psi)^{1/2} - B(1 - \alpha^2)\frac{p\sin^2\Psi}{(1 + \alpha^2\tan^2\Psi)^{1/2}} \quad \text{with} \quad A \sim 2.25, \quad B \sim 3.18. \tag{6}$$

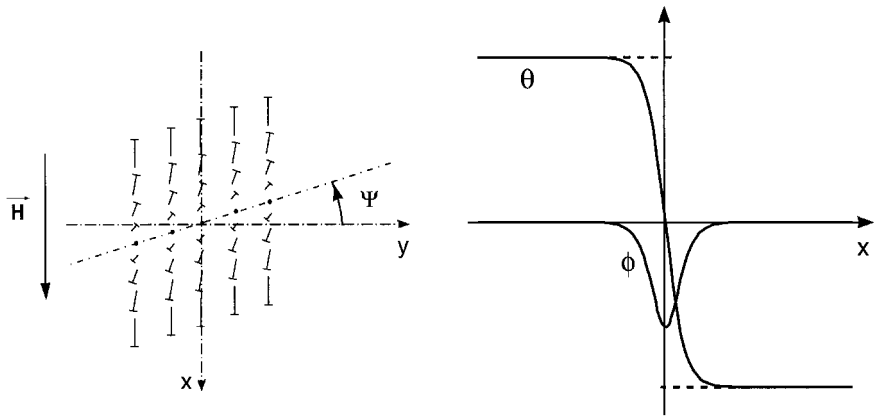

Figure 14. Definitions of θ and ϕ for an Ising wall turned of an angle Ψ. θ has been chosen with a hyperbolic form. The variation distances of θ and ϕ are assumed to be the same.

Downloaded At: 18:12 25 January 2011

The first term in equation (6) expresses the energy cost of the wall elongation due to its rotation. The second term accounts for the escape of the director from the (x, z) plane close to the interface. This escape introduces favourable elastic distortions inside the wall and consequently decreases the free energy of the wall.

The linearization of the free energy with respect to ϕ leads to the suppression of the term $\chi_a H^2 \phi^2 \sin \theta^2$. This term represents the restoring force towards the vertical magnetic plane exerted by the magnetic field. It is a positive energy term that disfavours the rotation of the wall. This term apparently corresponds to a second order effect in the destabilization and probably plays a role in the saturation of the instability.

For all values of the anisotropy α, the even function $f(\Psi)$ meets $f(0) = 0$ and $\lim_{\Psi \to \pm \pi/2} f(\Psi) = \infty$. For $\alpha = 1$ (isotropic case), the function $f(\Psi)$ is obviously a monotonically decreasing function of Ψ. For $\alpha < 1$, the sign of its second derivative determines the stability of the straight wall. Actually, for $f''(0) > 0$, the splay–bend configuration is stable, whereas for $f''(0) < 0$, this configuration becomes unstable; new minima at $\Psi \neq 0$ necessarily emerge in order to satisfy the divergence condition of the function $f(\Psi)$ at infinity. After a straightforward calculation, this derivative reads $f''(0) = A\alpha^2 - 2B(1 - \alpha^2)p$. For $\alpha < 1$, and under the assumption that p is small, one can have $f''(0) < 0$ for a strong enough anisotropy. Then, $\Psi = 0$ corresponds to a maximum of the free energy whereas at least two new minima appear in the interval $]-\pi/2; \pi/2[$. In figure 15, we have plotted the curve $f(\Psi)$ for Ψ ranging from $-\pi/2$ to $\pi/2$, and for two different values of the elastic anisotropy. The p value has been arbitrarily set at 0.02. The following values for the physical constants and control parameters have been used: $K = 7.4\,10^{-12}$ N (which is the average of the splay and bend constants given in § 2), $\chi_a = 1.142$, $\varepsilon_a = 11.3$, $H = 0.7$ T, $V_{\text{Peak-to-Peak}} = 22$ V and $d = 100\,\mu$m. With these values the width of the wall is $1/k = \xi \sim 4\,\mu$m.

The curves obtained indicate that there exists a critical value of the elastic anisotropy that yields the emergence of two new minima, at $\Psi = \pm \Psi_0$. This critical anisotropy, which defines the onset of the instability, is higher than the one deduced from the experiments. This discrepancy probably follows from the simplifying assumptions used in the energy model, which shift the threshold of the instability. The model still provides an explanation for the destabilization of the wall in terms of energy. For a sufficiently high value of the elastic anisotropy, the straight splay–bend Ising wall is unstable towards a tilted wall. Due to the translational invariance of the system along the y-axis (infinite medium), the destabilization leads to the simultaneous appearance of two new minima. This explains the formation of the zigzag interface. The conclusions drawn from this analysis are strengthened by direct minimization of the two-dimensional free energy using a numerical scheme (see figure 16). The coarsening dynamics that follows tends to separate the facets by suppressing the regions of high curvature of the interface which are energetically costly.

5. Conclusion

The existence of a new instability for a splay–bend Ising wall in a 5CB nematic liquid crystal has been emphasized. The origin of this instability lies in the elastic anisotropy of the nematic compound used ($K_2 < K_1, K_3$). Such a result is explained using a theoretical approach based on the nematic free energy. More precisely, the instability induces a change in the splay–bend wall structure allowing the appearance of some twist distortion. In a magnetic trap, the unstable Ising wall then reaches a steady periodic profile. In a different way, when the

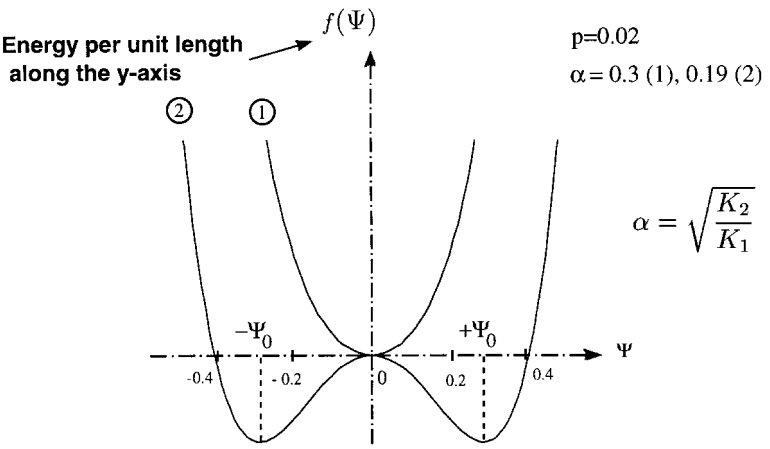

Figure 15. Free energy curves for a maximum out-of-plane quantified by $p = 0.02$ and for two different values of the elastic anisotropy α. For a strong enough anisotropy, the splay–bend Ising wall becomes unstable; two new minima appear at $\pm \Psi_0$ in place of the previous minimum at $\Psi = 0$.

Downloaded At: 18:12 25 January 2011

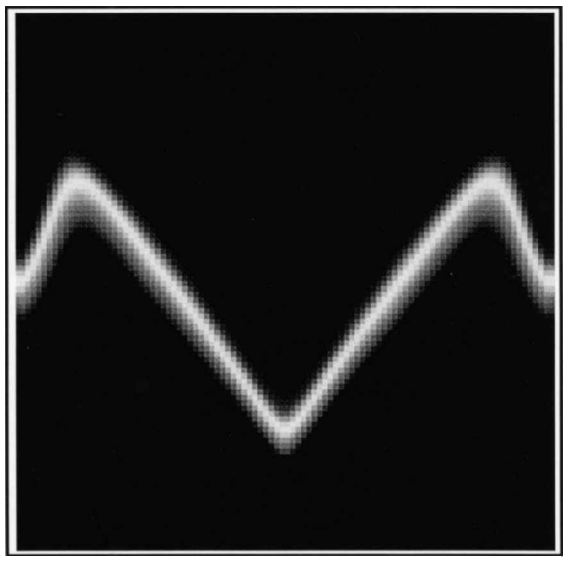

Figure 16. Numerical result obtained from a minimization of the free energy; the numerical scheme assumes that the problem is two-dimensional which means that θ and ϕ do not depend on z. Numerical parameters: $K_1 = K_3 = 7.10^{-12}$ N, $K_2 = 3.10^{-12}$ N, $\varepsilon_a = 11.3$, $\chi_a = 1.142$ (10^{-7} cm^3 g^{-1}), $H = 0.8$ T, $V_{PtoP} = 32.7$ V.

magnetic field is homogeneous, the interface undergoes a spinodal decomposition into facets. In both cases, the unstable state has been experimentally characterized.

We would like to thank Lionel Gil who has developed the numerical scheme for the minimization of the free energy.

Downloaded At: 18:12 25 January 2011

References

[1] De Gennes, P. G., and Prost, J., 1993, *The Physics of Liquid Crystals* (Oxford: Clarendon Press).
[2] Lonberg, F., and Meyer, R. B., 1985, *Phys. Rev. Lett.*, **55,** 718; Srajer, G., Lonberg, F., and Meyer, R. B., 1991, *Phys. Rev. Lett.*, **67,** 1102; Miraldi, E., Oldano, C., and Strigazzi, A., 1986, *Phys. Rev. A*, **34,** 4348; Barbero, G., Miraldi, E., and Oldano, C., 1988, *Phys. Rev. A*, **38,** 519; Kini, U. D., 1986, *J. Physique*, **47,** 693.
[3] Cladis, P. E., and Torza, S., 1975, *J. appl. Phys.*, **46,** 584.
[4] Chandrasekhar, S., 1992, *Liquid Crystals* (Cambridge: University Press), cover page.
[5] Chevallard, C., Gilli, J.-M., Frisch, T., Chikina, I. V., and Pieranski, P., 1999, *Mol. Cryst. liq. Cryst.*, **328,** 595 (Proceedings of the XVIIth International Liquid Crystal Conference).
[6] Nobili, M., 1998, private communication.
[7] Gilli, J.-M., 1995, private communication.
[8] Vierheilig, A., Chevallard, C., and Gilli, J.-M., 1997, *Phys. Rev. E*, **55,** 7128.
[9] Galerne, Y., and Lièbert, L., 1985, *Phys. Rev. Lett.*, **55,** 2449; Galerne, Y., Itoua, J., and Lièbert, L., 1988, *J. Phys. Fr.*, **49,** 681.
[10] Brochard, F., 1972, *J. Phys. (Paris)*, **33,** 607.
[11] Zimmermann, W., and Kramer, L., 1985, *Phys. Rev. Lett.*, **55,** 402; Ribotta, R., Joets, A., and Lei, L., 1986, *Phys. Rev. Lett.*, **56,** 1595.
[12] Schmiedel, H., Cramer, Ch., Stannarius, R., Eidner, K., and Grigutsch, M., 1993, *Liq. Cryst.*, **14,** 1935; Cramer, Ch., Kühnau, U., Schmiedel, H., Stannarius, R., 1994, *Mol. Cryst. liq. Cryst.*, **257,** 99.
[13] Manneville, P., and Piquemal, J.-M., 1983, *Phys. Rev. A*, **28,** 1774; Cross, M. C., and Hohenberg, P. C., 1993, *Rev. Mod. Phys.*, **65,** 859.
[14] Ribotta, R., Joets, A., and Lei, L., 1986, *Phys. Rev. Lett.*, **56,** 1595; Bodenschatz, E., Kaiser, M., Kramer, L., Pesch, W., Weber, A., and Zimmermann, W., 1990, *New Trends in Nonlinear Dynamics and Pattern-Forming Phenomena*, edited by P. Coullet and P. Huerre (New York: Plenum Press).
[15] Golovin, A. A., Davis, S. H., and Nepomnyashchy, A. A., 1998, *Physica D*, **122,** 202.
[16] Melo, F., and Oswald, P., 1991, *Ann. Chim. Fr.*, **16,** 236.
[17] Limat, L., 1998, *Europhys. Lett.*, **44,** 205.
[18] Chevallard, C., Clerc, M., Coullet, P., and Gilli, J.-M., 2000, *Eur. Phys. J. E*, **1,** 179; Chevallard, C., Clerc, M., Coullet, P., and Gilli, J.-M., *Phys. Rev. Lett.* (submitted).
[19] Helfrich, W., 1968, *Phys. Rev. Lett.*, **21,** 1518.
[20] Gilli, J.-M., Morabito, M., and Frisch, T., 1994, *J. Phys. II Fr.*, **4,** 319.
[21] Bradshaw, M. J., Raynes, E. P., Bunning, J. D., and Faber, T. E., 1985, *J. Phys. (Paris)*, **46,** 1513; Coles, H. J., and Sefton, M. S., 1985, *Mol. Cryst. liq. Cryst.*, **1,** 151.
[22] Ratna, B. R., and Shashidhar, R., 1977, *Mol. Cryst. liq. Cryst.*, **42,** 113.
[23] Sherrell, P. L., and Crellin, D. A., 1979, *J. Phys. Colloq.*, **C3,** 40.
[24] Figueiredo Neto, A. M., Martinot-Lagarde, Ph., and Durand, G., 1984, *J. Phys. Lett.*, **45,** 793.
[25] Cahn, J. W., and Hilliard, J. E., 1958, *J. chem. Phys.*, **28,** 258.